

Phase-shift anomaly caused by subwavelength-scale metal slit or aperture diffraction

Kanghee Lee,¹ Minwoo Yi,¹ Sang Eon Park,² and Jaewook Ahn^{1,*}

¹Department of Physics, KAIST, Daejeon 305-701, South Korea

²Korea Research Institute of Science and Standards, Daejeon 305-340, South Korea

*Corresponding author: jwahn@kaist.ac.kr

Received November 5, 2012; revised December 3, 2012; accepted December 7, 2012;
posted December 11, 2012 (Doc. ID 179300); published January 9, 2013

Terahertz time-domain spectroscopy probes anomalous phase-shift caused by wave diffraction from a subwavelength-scale metal slit or aperture. Carrier frequency phase measurements in the far-field region reveals that nearly 30° phase advance is induced from a subwavelength slit diffraction and that 180° phase-advance from a subwavelength aperture. These results indicate that the conventional 90° phase advance of diffracted waves in the far-field region, known as the Gouy phase shift, is not valid for subwavelength diffraction phenomena. The physical origin of these phase-shift anomalies is attributed to induced electric currents or magnetic dipole radiation, and theoretical analyses based on these factors are in good agreement with the experimental results. © 2013 Optical Society of America

OCIS codes: 050.1940, 050.5080, 050.6624, 300.6495.

Wave diffraction through an aperture is well explained by Kirchhoff's scalar diffraction theory when the size d of the aperture is large compared to the wavelength λ of the wave [1]. However, as Bethe pointed out, the diffraction phenomena from a subwavelength-sized aperture (i.e., $d \ll \lambda$) are not consistent with this scalar diffraction theory [2], and subwavelength aperture transmission has been an important research subject ever since. Furthermore, the recent emergence of near-field optical applications and subwavelength-resolution imaging has created additional motivation to better understand subwavelength diffraction phenomena in various experimental situations [3–5]. Some examples include subwavelength transmission intensities, propagation distributions, local field enhancements, and so on [6–10]. There have also been recent reports on extraordinary field enhancement of subwavelength slit aperture diffraction due to large accumulations of charges near the slit edges [11,12]. Nevertheless, of particular relevance to the context of this Letter, phase study of subwavelength aperture diffraction has been virtually ignored. We note that phase information on electromagnetic waves is of particular importance since electromagnetic waves of a few cycles, or even sub-cycle waves, are used in various research areas [13–17].

In this Letter, we report a phenomenological theory for subwavelength diffraction phase-shift anomaly and verify its predictions by direct phase measurement in terahertz (THz) time-domain experiments. We use two types of test geometries (a slit and a circular aperture), both on a subwavelength scale, and diffraction phase shift is investigated as a function of the geometrical factors.

Let us consider that a monochromatic plane wave of angular frequency ω , propagating along the z direction, diffracts through an aperture located at $z = 0$. When the aperture is a perfect conductor and large enough that the aperture edge effect can be ignored, then according to Kirchhoff's scalar diffraction theory [1], the diffracted wave in the far-field region at $\vec{R} = (X, Y, Z)$ is given by

$$\vec{E}_T(\vec{R}) = -i \frac{k e^{ikR}}{2\pi R} \iint \vec{E}_0 e^{-ik\frac{rX+yY}{R}} \mathcal{O} dx dy, \quad (1)$$

where E_T represents the diffraction of the transmitted wave, Σ denotes the aperture plane, \mathcal{O} the obliquity factor, E_0 the incident electric field amplitude, $k = \omega/c$, and $R = |\vec{R}|$. The 90° phase-advance of $E_T(\vec{R})$, with respect to the e^{ikR} phase factor of plane-wave propagation, is caused by transverse wave confinement through the aperture and is generally known as the Gouy phase shift, which we denote by ϕ_G [18–21].

However, when a subwavelength aperture is used, the diffracted field is affected by the induced electric currents at the aperture edges and the scalar diffraction theory based on Eq. (1) fails. The induced electric field can be obtained from the vector potential $\vec{A}(\vec{R})$, given by

$$\vec{A}(\vec{R}) = \frac{\mu_0 e^{ikR}}{4\pi_0 R} \iint_{\Sigma} \vec{J}(x, y) e^{-ik\frac{rX+yY}{R}} dx dy, \quad (2)$$

where $\vec{J}(x, y)$ is the current density and μ_0 is the magnetic permeability. The induced currents should satisfy proper boundary conditions on the aperture edge, and the phase of the induced electric field is determined by these currents. Therefore, the diffracted electric field could be phase-shifted.

As our first example, we consider the diffraction from a slit of subwavelength width d , shown in Fig. 1. In the presence of an incident electric field with a time-varying phase factor $e^{-i\omega t}$ on the metal surfaces around the slit, a pair of opposite charges are accumulated in the phase

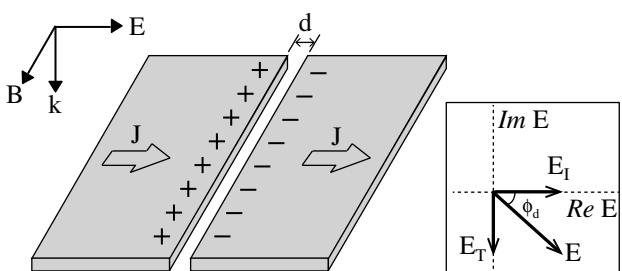


Fig. 1. Schematic of subwavelength slit diffraction. The inset shows a vector addition diagram for diffracted electric fields.

with the electric field, in accordance with Gauss law. Then, within the slit an electric current density \vec{J}_{slit} is induced, and its time variation is phase-shifted from the incident electric field according to $\vec{J}_{\text{slit}}/|\vec{J}_{\text{slit}}| = -i\vec{E}_0/|\vec{E}_0|$. In the far-field diffraction region, therefore, the diffraction of the induced electric field \vec{E}_I is obtained from Eq. (2) by

$$\vec{E}_I(\vec{R}) = \frac{ck\mu_0 e^{ikR}}{4\pi R} \int_C \vec{E}_0 e^{-ik\frac{px+qy}{R}} \mathcal{Q}_a(\lambda) ds, \quad (3)$$

where C is the integration path around the aperture and $\mathcal{Q}_a(\lambda)$ denotes the corresponding geometrical correction which is proportional to wavelength λ in the slit diffraction according to the λ -zone theory [12]. Note that the induced electric field contribution \vec{E}_I in Eq. (3) is phase-shifted by 90° from the transmitted electric field contribution \vec{E}_T in Eq. (1). Thus, the net diffracted electric field, or the sum of the two contributions from Eqs. (1) and (3), can be represented in the complex plane, as shown in the inset of Fig. 1, and the phase-shift anomaly caused by diffraction (or the diffraction phase) can be defined along the optical axis (i.e., $x = y = 0$) as

$$\phi_d = \tan^{-1} \frac{E_T}{E_I}. \quad (4)$$

Also note that the geometrical scaling of \vec{E}_T is proportional to d/λ , while the induced field \vec{E}_I is constant regardless of d . Therefore, the phase-shift ϕ_{slit} in Eq. (4) satisfies the relationship

$$\phi_{\text{slit}} = \tan^{-1} \frac{\alpha d}{\lambda}, \quad (5)$$

where α is a constant. As a result, the contribution of the induced electric field to the diffraction phase gradually becomes significant in the subwavelength diffraction regime and the diffraction phase ϕ_d changes accordingly, from 90° (the normal Gouy phase shift) to 0° in the limit of extreme subwavelength-sized slit transmission.

Experimental verification of the phase-shift anomaly for subwavelength slit diffraction was performed with the waveform capture technique in THz time-domain spectroscopy [22]. We used a photoconductive antenna for generation, and an electro-optical sampler with a $\langle 110 \rangle$ ZnTe crystal, 2 mm thick, for detection in a 100 MHz Ti:sapphire laser oscillator system. The diffraction slits were located at the focus of the THz-TDS in an 8 f geometric configuration. A conventional circuit board manufacturing technique was used to pattern single slits of width d on a thin copper sheet, 18 μm thick, on a polytetrafluoroethylene plate with a thickness of 0.8 mm. We tested 16 different slit widths, ranging from $d = 100$ to 700 μm in 40 μm increments. After Fourier transform analysis of the temporal traces of THz waves through the slits, we obtained frequency-dependent direct phase measurements in the frequency range from 0.1 to 1 THz. The experimental geometry and results from the series of single slits are summarized in Fig. 2. We observed a gradual increase in the temporal delay of the peak of the waveform as the width of the slit d decreases from the largest to the smallest value. The phase shifts extracted from a set of selected frequency components

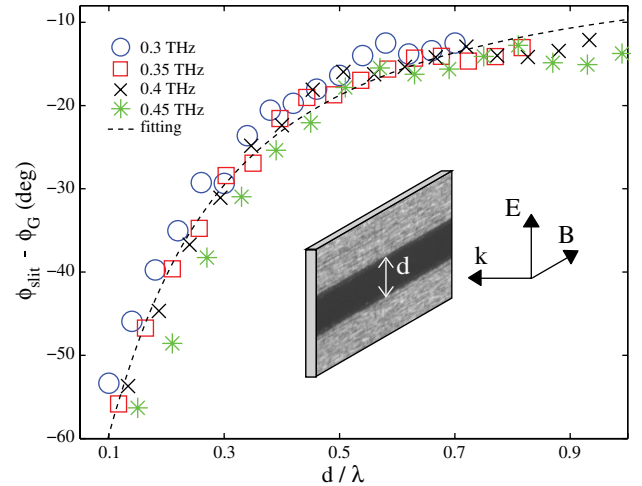


Fig. 2. (Color online) Measured phase shifts from subwavelength-scale slits. The phase shifts $\phi_{\text{slit}} - \phi_G$ are measured for 0.3, 0.35, 0.4, and 0.45 THz. The black dashed curve represents a fit based on Eq. (5). The inset figure is an optical microscopic image of a slit and the directions of the E and B fields, and momentum.

(0.3, 0.35, 0.4, and 0.45 THz) of the Fourier-transformed experimental data are plotted with various symbols in Fig. 2. All phases are compared with the normal Gouy phases ϕ_G , which are measured using a bare polytetrafluoroethylene plate. The phase-shift changes as d/λ decreases in good agreement with the theory.

As a second example, we now consider the diffraction from a circular aperture on a subwavelength scale. The same procedure used in the first experiment was applied to a series of circular apertures. We tested 16 different hole radii, ranging from $a = 100$ to 475 μm in 25 μm increments. From the experimental results summarized in Fig. 3, we observe that the peak gradually advances for smaller apertures, which is opposite to what was observed in the slit experiment. First, the electric fields from two-dimensional subwavelength apertures are typically very weak compared to the incident electric fields (unlike the electric field enhancement of a slit), because

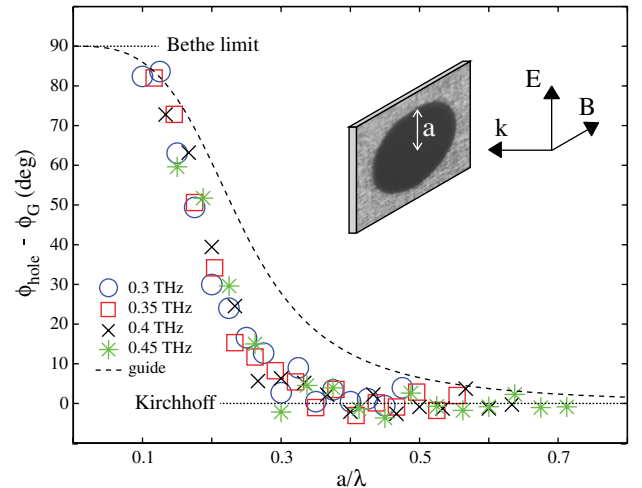


Fig. 3. (Color online) Measured data from subwavelength circular hole diffraction. The phase shifts $\phi_{\text{hole}} - \phi_G$ are measured at 0.3, 0.35, 0.4, and 0.45 THz. The dashed curve is the theoretical fit from Eq. (6).

the tangential component of the electric field on metal is zero, and thus the phase shift ordinarily expected from the electric field shielding in metal does not generalize to these types of apertures. Hence, we employ another physical interpretation for these types of apertures. At the limit of extreme subwavelength-sized aperture transmission, it is expected that the diffracted electric field is the radiation from an effective magnetic dipole \vec{m} , and \vec{m} should satisfy the relationship [1,2] as $\vec{m}/|\vec{m}| = -\vec{H}_0/|\vec{H}_0|$. In a far-field observation, the induced electric field \vec{E}_I should satisfy $\vec{E}_I \propto -\vec{k} \times \vec{m}$, and \vec{E}_I satisfies $\vec{E}_I \propto -\vec{E}_0$. Accordingly, the diffraction phase ϕ_d changes from 90° (the normal Gouy phase shift) to 180° in the limit of extreme subwavelength-sized circular aperture transmission. So, the observed phase advancement is consistent with the expectation for the limiting case of subwavelength circular aperture diffraction. From a more quantitative perspective, we can calculate the phase shift of circular hole diffraction with the help of both Bethe's formal work [2] and the following optical theorem [1], which relates the total cross section σ_t to the amplitude of the forward scattering field:

$$\sigma_t = \frac{4\pi}{k} \text{Im}[f(k = k_0)],$$

where $\text{Im}[f(k = k_0)]$ is the imaginary part of diffracted field that Bethe did not consider. In the small-aperture limit, $\sigma_t = 128k^4a^6/27\pi$ [2], so that this imaginary part becomes $32a^6k^5/27\pi^2R$. Also, according to Bethe [2], the real part of the diffracted field satisfies $4a^3k^2/3\pi R$. Hence, the phase shift of subwavelength diffraction can be expressed by

$$\phi_{\text{hole}} = \phi_G + \tan^{-1} \frac{9\lambda^3}{64\pi^2 a^3}. \quad (6)$$

The dashed curve in Fig. 3 represents the theoretical predictions based on Eq. (6).

It is worthwhile mentioning that our previous study of THz wave propagation from subwavelength emitters also dealt with the aperture-size dependence of the Gouy phaseshift in the subwavelength diffraction regime, where the observed temporal phase shift was explained by the subwavelength spatial confinement of the propagated wave [17]. However, the experimental conditions for the subwavelength emitters (a transient Dember dipolar field forced on a semiconductor film with a 45° tilt) were not sufficiently generalized for the conventional subwavelength diffraction problem considered in the present work.

In summary, we have considered phase-shift anomalies caused by subwavelength diffraction, using a time-domain wave-profile measurement technique. For slits or apertures of various subwavelength sizes, the phase-

shift was measured as a function of the slit or aperture size and the wavelength of the incident THz waves. The measured results indicate that slits induce a phase given by $\tan \phi_{\text{slit}} \propto -\lambda/d$, and holes given by $\tan(\phi_{\text{hole}} - \phi_G) = 9\lambda^3/64\pi^2 a^3$ under the subwavelength diffraction condition. So, at the limit of extreme subwavelength diffraction from a slit (an aperture), the diffracted wave is phase-advanced by 0° (180°), which differs from the constant 90° phase advancement, the Gouy phase shift. The physical origin of these phase-shift anomalies is attributed to the electric field originated from the induced currents or magnetic dipole radiation.

This work was supported in part by Basic Science Research Programs (2009-0090843, 2010-0013899, 2009-0083512) and in part by WCI Program (WCI 2011-001) through the National Research Foundation of Korea.

References

1. J. D. Jackson, *Classical Electrodynamics* 3rd ed. (Wiley, 1999).
2. H. A. Bethe, Phys. Rev. **66**, 163 (1944).
3. T. W. Ebbesen, H. J. Lezec, H. F. Ghaemi, T. Thio, and P. A. Wolff, Nature **391**, 667 (1998).
4. R. C. Dunn, Chem. Rev. **99**, 2891 (1999).
5. H. W. Kihm, S. M. Koo, Q. H. Kim, K. Bao, J. E. Kihm, W. S. Bak, S. H. Eah, C. Lienau, H. Kim, P. Nordlander, N. J. Halas, N. K. Park, and D.-S. Kim, Nat. Commun. **2**, 451 (2011).
6. C. J. Bouwkamp, Rep. Prog. Phys. **17**, 35 (1954).
7. C. Huang, R. D. Kodis, and H. Levine, J. Appl. Phys. **26**, 151 (1955).
8. Y. Nomura and S. Katsura, J. Phys. Soc. Jpn. **10**, 285 (1955).
9. C. Obermüller and K. Karrai, Appl. Phys. Lett. **67**, 3408 (1995).
10. D. J. Shin, A. Chavez-Pirson, S. H. Kim, S. T. Jung, and Y. H. Lee, J. Opt. Soc. Am. A **18**, 1477 (2001).
11. M. A. Seo, H. R. Park, S. M. Koo, D. J. Park, J. H. Kang, O. K. Suwal, S. S. Choi, P. C. M. Planken, G. S. Park, N. K. Park, Q. Park, and D. S. Kim, Nat. Photonics **3**, 152 (2009).
12. J. H. Kang, D. S. Kim, and Q. Park, Phys. Rev. Lett. **102**, 093906 (2009).
13. G. G. Paulus, F. Grasbon, H. Walther, P. Villoresi, M. Nisoli, S. Stagira, E. Priori, and S. De Silvestri, Nature **414**, 182 (2001).
14. D. J. Jones, S. A. Diddams, J. K. Ranka, A. Stentz, R. S. Windeler, J. L. Hall, and S. T. Cundiff, Science **288**, 635 (2000).
15. T. Brabec and F. Krausz, Rev. Mod. Phys. **72**, 545 (2000).
16. K. Lee and J. Ahn, Appl. Phys. Lett. **97**, 241101 (2010).
17. M. Yi, K. Lee, J. D. Song, and J. Ahn, Appl. Phys. Lett. **100**, 161110 (2012).
18. L. G. Gouy, C. R. Acad. Sci. Paris **110**, 1251 (1890).
19. A. E. Siegman, *Lasers* (University Science Books, 1986).
20. S. Feng and H. G. Winful, Opt. Lett. **26**, 485 (2001).
21. N. C. R. Holme, B. C. Daly, M. T. Myaing, and T. B. Norris, Appl. Phys. Lett. **83**, 392 (2003).
22. D. Grischkowsky, S. Keiding, M. van Exter, and Ch. Fattinger, J. Opt. Soc. Am. B **7**, 2006 (1990).